On the electronic structure of some mono- and bisoxazolines

Branka Kovač,* Leo Klasinc, Zlata Raza and Vitomir Šunjić

The "Ruđer Bošković" Institute, HR 10 001 Zagreb, POB 1016, Croatia

Received (in Cambridge, UK) 26th July 1999, Accepted 20th September 1999

He(I) photoelectron (PE) spectra of 2-methyl-4,5-dihydro-1,3-oxazole **1**, 4-(*tert*-butyl)-2-{[4-(*tert*-butyl)-4,5-dihydro-1,3-oxazol-2-yl]methyl}-4,5-dihydro-1,3-oxazole **2**, 4-(*tert*-butyl)-2-{1-[4-(*tert*-butyl)-4,5-dihydro-1,3-oxazol-2-yl]-1-methylethyl}-4,5-dihydro-1,3-oxazole **3**, 4-phenyl-2-[(4-phenyl-4,5-dihydro-1,3-oxazol-2-yl)methyl]-4,5-dihydro-1,3-oxazole **4**, 2-[1-methyl-1-(4-phenyl-4,5-dihydro-1,3-oxazol-2-yl)ethyl]-4-phenyl-4,5-dihydro-1,3-oxazole **5**, 2-(4-isopropyl-4,5-dihydro-1,3-oxazol-2-yl)phenol **6**, *N*-phenyl-*N*-[2-(4-phenyl-4,5-dihydro-1,3-oxazol-2-yl)phenyl]amine **7**, *N*-methyl-*N*-[2-(4-phenyl-4,5-dihydro-1,3-oxazol-2-yl)phenyl]amine **8**, *N*,*N*-diphenyl-*N*-[2-(4-phenyl-4,5-dihydro-1,3-oxazol-2-yl)phenyl]amine **9**, and *N*-[2-(4-isopropyl-4,5-dihydro-1,3-oxazol-2-yl)phenyl]-*N*,*N*-diphenylamine **10** have been recorded and their valence electronic structures analysed using quantum chemical *ab initio* and/or PM3 calculations. Also, a discussion of IR, UV spectra and a correlation of ^{13}C NMR chemical shifts with total atomic charges are presented.

Introduction

Chiral oxazoline ligands are ubiquitous in organometallic complexes, which catalyse various asymmetric reactions. They can act as mono-, bi- or tridentate 1,4- or 1,5-nitrogen ligands, depending on the number of oxazoline rings, alone or in combination with other heteroatom-containing units present in the chiral polydentate ligand. Such 1,5-N,X-ligands can be represented by the general formulae I–III. It is important to note

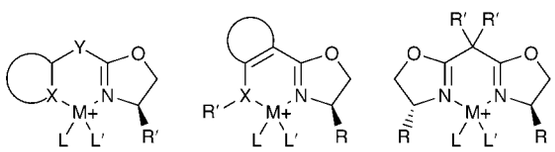

I II III

X = N, P, S, O
Y = CH_2, NR′

that the bidentate ligand comprises either a conjugated 4π system, as in II, or such conjugation takes place upon enolization into enamine form. This form is possible for III if R′ = H.

Among the most explored catalytic complexes with chiral ligands are those with Cu(I) that catalyse enantioselective cyclopropanation of alkenes[1–4] and other carbon–carbon bond forming reactions,[5,6] Rh(II) complexes which catalyse allylation of aldehydes,[7] Pd(I) complexes that catalyse allylic substitution,[8–14] Ir(I) complexes for asymmetric Wacker-type cyclization,[15] Ru(II)[16] and Ti(IV) complexes[17] that catalyse hydrogenation of inactivated alkenes.

Enantioselectivity of organometallic ligands is determined by the chiral topology of the catalytic complex, whereas the electronic structure is of utmost importance for completion of the catalytic cycle. Catalytic efficacy of chiral complexes with nitrogen ligands is generally determined by their dynamic stability. In particular it depends on the ability of the central metal atom to change its coordination number and its oxidation state, and on the relative stability of the catalyst–product *vs.* catalyst–reactant complex. The latter properties are mainly determined by the stereoelectronic characteristics of the ligand; in particular by the electron-donating ability of the coordinated nitrogen atom.

In order to obtain more information about the stereoelectronic structure of chiral oxazolines which form an important class of 1,5-dinitrogen ligands, we initiated a study of the electronic structures of mono- (**1**,[18] **6**–**10**[19]) and bis-oxazolines (**2**–**5**)[18] by PE spectroscopy in combination with *ab initio* 6-31G* (for **1**–**3**) and/or semiempirical PM3 quantum-chemical calculations[20] (for **1**–**10**). We have also taken into consideration the information provided by UV and ^{13}C-NMR spectra.

Experimental

The He(I) PE spectra were recorded on a Vacuum Generators UV-G3 photoelectron spectometer[21] with a spectral resolution of 25 meV, measured as the full width at half maximum (FWHM) of the Ar^+ $^2P_{3/2}$ calibration line. The sample inlet temperatures required to generate sufficient sample vapour pressure were 25, 80, 80, 180, 150, 80, 170, 130, 180 and 130 °C for **1**–**10** respectively. The energy scale was calibrated by addition of a small amount of Xe to the sample gas flow.

The electronic structure calculations were performed by the MOPAC 7.0 program package using a PM3 model Hamiltonian and the GAUSSIAN94 program package.[20]

NMR spectra were recorded in $CDCl_3$ and CD_3OD on a Varian XL-300 GEM spectrometer using TMS as internal standard.

UV spectra were recorded on a Philips PU 8730 UV/VIS spectrometer (in MeOH and/or CCl_4).

Compounds **1**–**5** were purchased from a commercial source (Aldrich), and **6**–**10** were prepared and purified as described in ref. 19.

Results and discussion

The common constituent of all the studied compounds is an oxazoline moiety and we have therefore measured and analysed the photoelectron spectrum of 2-methyl-4,5-dihydro-1,3-oxazole **1** (Fig. 1) which can thus serve as a reference molecule. In the low energy region of its spectrum (<12 eV) two band systems appear with vertical ionization energies at 9.45 and 10.23 eV. According to PM3 and *ab initio* 6-31G* calculations, the first ionization energy should be ascribed to a $\pi_{C=N}$ ionization (**1** HOMO) (see Table 1), whereas the second system has its origin in electron ionization from a nitrogen lone-pair orbital (**1** SHOMO). The measured energy splitting, $\Delta E_{1,2}$, amounts to 0.78 eV; which is more consistent with PM3 (0.77 eV) than with *ab initio* 6-31G* (1.46 eV) results (Table 1).

Table 1 Vertical ionization energies (E_i/eV) and orbital energies (PM3 and *ab initio* 6-31G*) for highest occupied levels for **1**

	$-\varepsilon_i$/eV	
E_i/eV	PM3	*ab initio* 6-31G*
9.45 [1200 ± 80 cm^{-1}]	9.89 π_{CN}	10.055 π_{CN}
10.23	10.66 n_N	11.515 n_N
12.5	12.36 π_{OCN}	13.758 n_O
	13.46 n_O	13.883 π_{OCN}

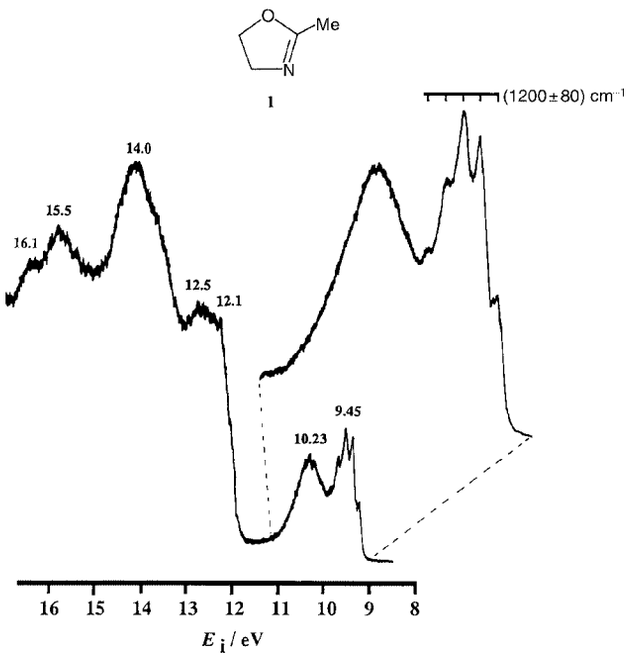

Fig. 1 He(I) PE spectrum of **1**.

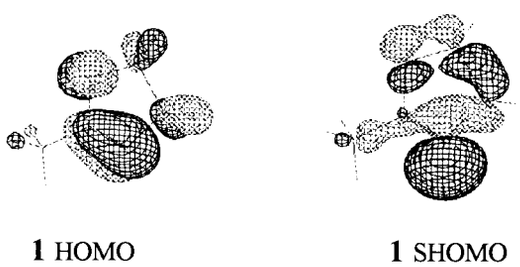

The resolved vibrational fine structure [$\tilde{\nu}_{CN}$ = 1200 ± 80 cm^{-1}] in the first band can be considered as an experimental confirmation of such an assignment, since it can be attributed to the C–N stretching mode. It is interesting to note that in PE spectra of many acyclic and cyclic imines, both with exo-[22] and endocyclic C=N bonds in heterocyclic rings,[23] the band with the lowest ionization energy is ascribed to electron ejection from an n_N rather than a $\pi_{C=N}$ orbital. The assignment of the first ionization energy in **1** to $\pi_{C=N}$ electron ejection, is a crucial argument for the present interpretation of the PE spectra of both symmetric (**2**–**5**) and unsymmetric (**6**–**10**) oxazolines.

Bisoxazolines

The low energy region of the PE spectra of the C_2-symmetric bisoxazolines **2**–**5** is shown in Fig. 2. Special attention is paid to bands corresponding to ionization energies below ~12 eV, since the coordinating ability in their metal complexes is expected to correlate with the lowest ionization energies.[24] The assignment is again based on *ab initio* 6-31G* and/or semiempirical PM3 calculations together with the earlier assignments for **1**.

The general appearance of the PE spectrum of **2** resembles

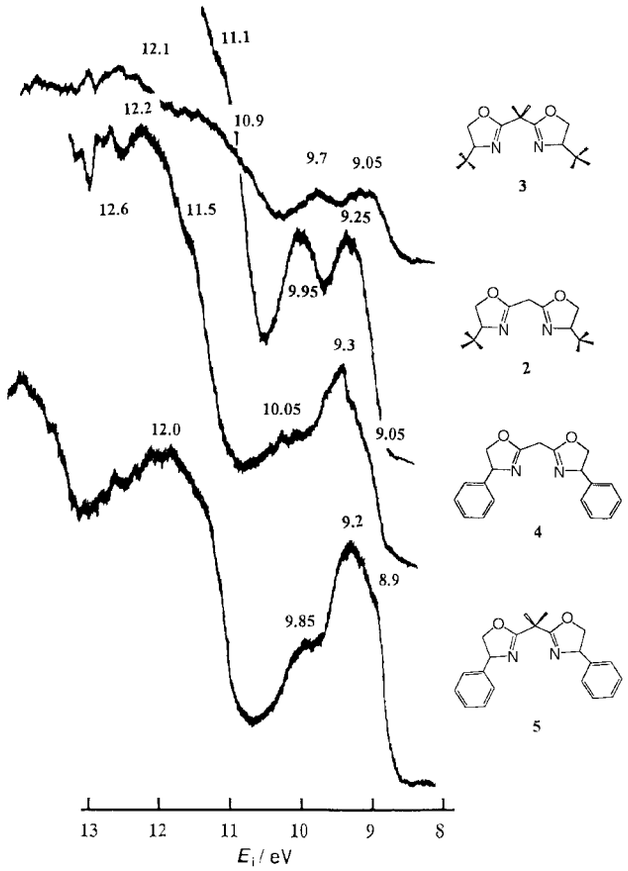

Fig. 2 He(I) PE spectra of **2**–**5**.

that of **1** except for the absence of resolved vibrational structure in the first band. Both *ab initio* and semiempirical PM3 calculations predict that the first Franck–Condon (FC) envelope of **2** results from two overlapping, nearly degenerate bands of $\pi_{C=N}$, and the second band arises from two linear combinations of n_N parentage (Table 2, and orbital diagrams below). This overlap can explain the absence of fine structure in the first band of **2**.

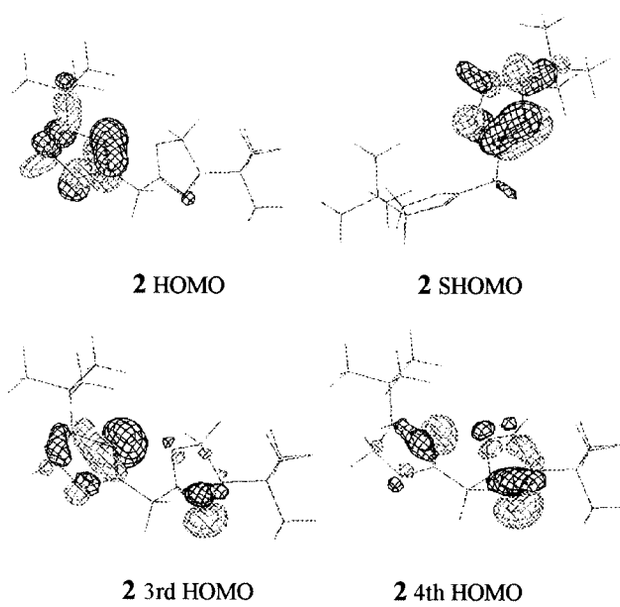

It also implies that the two $\pi_{C=N}$ and two n_N orbitals mix only negligibly, being too far apart energetically for significant through-bond (TB) interaction, and not being spatially aligned for through-space (TS) interactions.[25] Both the energy differences between the maxima of the two lowest ionization energy

Table 2 Vertical ionization energies (E_i/eV) and orbital energies for highest occupied levels for **2**–**5**[a]

Compound	ε_i/eV	$-\varepsilon_i$/eV PM3	$-\varepsilon_i$/eV *ab initio* 6-31G*
2	9.25	9.95 π_{CN}	9.893 π_{CN}
		10.07 π'_{CN}	10.103 π'_{CN}
	9.95	10.63 $n_N - n'_N$	11.319 $n_N - n'_N$
		10.64 $n_N + n'_N$	11.431 $n_N + n'_N$
3	9.05	9.92 π_{CN}	9.823 π_{CN}
		9.93 π'_{CN}	10.011 π'_{CN}
	9.7	10.53 $n_N - n'_N$	11.216 $n_N - n'_N$
		10.56 $n_N + n'_N$	11.307 $n_N + n'_N$
4	9.05	9.61 π^s_b	
		9.66 $\pi^s_{b'}$	
	9.3	9.79 π^a_b	
		9.80 $\pi^a_{b'}$	
		10.05 $\pi_{CN} - \pi'_{CN}$	
		10.18 $\pi_{CN} + \pi'_{CN}$	
	10.05	10.73 n_N	
		10.76 n'_N	
5	8.9	9.60 π^s_b	
		9.61 π^s_b	
	9.2	9.76 π^a_b	
		9.79 $\pi^a_{b'}$	
		9.98 $\pi_{CN} - \pi'_{CN}$	
		10.15 $\pi_{CN} + \pi'_{CN}$	
	9.85	10.61 n_N	
		10.69 n'_N	

[a] In the case of two identical substituents or constituent parts in the molecule, the hyphenated MO corresponds to their less stable combination.

Table 3 UV data for **1**–**3**

Compound	ε_{max}/L mol^{-1} cm^{-1}	λ_{max}/nm
1 (MeOH)	295	214
2 (MeOH)	5275	206
	976	278
2 (CCl_4)	1095	269
3 (MeOH)	264	216

FC envelopes (0.78 and 0.70 eV, in **2** and **1**, respectively), and the corresponding band widths are almost the same, thus supporting the proposed degeneracy of these systems.[26]

The structure of **2** suggests the presence of tautomeric forms, **2a** and **2b**, which differ in the location of a hydrogen atom and in the possibility for 4π conjugation in **2b**, Scheme 1. However,

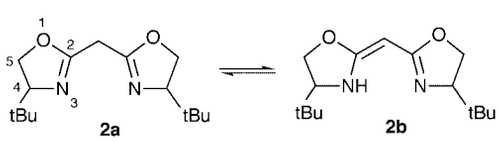

Scheme 1

the PE spectrum reveals the structure of bisoxazoline **2a** to be the preferred tautomer in the gas phase.

This interpretation is confirmed by the PE spectrum of **3**, which is almost identical to **2** except for the expected inductive shift towards lower ionization energies due to the presence of methyl groups. Unlike **2**, there is no possibility for imine–enamine tautomerism in **3**.

It is well known that the tautomeric equilibrium and hydrogen shifts could be strongly influenced by the polarity of the surrounding medium.[27] Therefore, NMR (both ^{1}H and ^{13}C) and UV spectra have also been measured.

The ^{1}H-NMR spectrum (in $CDCl_3$) shows the presence of CH_2 in the bridge ($\delta_{C(2)-CH_2}$ = 3.35 for **2** and 3.56 for **4**) and no signal that might be attributed to C(2)–C**H** and N**H** groups. ^{13}C-NMR spectra also show the presence of CH_2 in the bridge ($\delta_{C(2)-CH_2}$ = 28.06 for **2** and 28.00 for **4**) and of N=**C**(2) [$\delta_{C(2)}$ = 161.55 for **2** and 162.98 for **4**]. The quantitative ^{13}C-NMR spectrum of **2**, recorded in CD_3OD, shows the presence of tautomer **2a** only. Besides, because of the reduction in symmetry on going from **2a** to **2b**, the number of signals in ^{13}C-NMR should increase, which was not observed. Thus, tautomer **2a** is evidently the dominant species in the gas phase as well as in solution.

Comparison of UV spectra of **1**–**3** in solution gives some interesting results (Table 3): the spectrum of **1** exhibits one absorption band only, with ε_{max} = 295 L mol^{-1} cm^{-1} at 214 nm, which is tentatively assigned to a $\pi^*_{CN} \leftarrow \pi_{CN}$ transition. In the spectrum of **2**, however, two bands were observed. The shorter-wavelength electronic absorption at 206 nm has significantly larger intensity as compared to **1**: ε_{max} = 5275 L mol^{-1} cm^{-1}. The additional absorption transition in the lower energy range, λ_{max} = 278 nm, is much weaker (ε_{max} = 976 L mol^{-1} cm^{-1}) (see Table 3). The enhancement of the transition ascribed to a $\pi^*_{CN} \leftarrow \pi_{CN}$ transition could be rationalized by some kind of intramolecular charge transfer (between the n_N of one oxazoline ring and the $\pi_{C=N}$ of the other),[28–30] rather than by interaction with the solvent. The former effect is transmitted by the high p-character of the partial anionic C-atom in the bridging CH_2-group, *i.e.* by a hyperconjugative effect. The additional long-wavelength absorption could be the result of an electronic transition attributed to the **2b** tautomeric form which has a π-conjugated system, giving rise to the bathochromic shift relative to the $\pi^*_{CN} \leftarrow \pi_{CN}$ transition of **2a**. In nonpolar CCl_4 this absorption band in **2** is shifted to a lower wavelength (λ_{max} = 269 nm) but its intensity is not affected [ε_{max}/L mol^{-1} cm^{-1} = 1095]. We believe the hypsochromic shift to be the reason for the absence of a $\pi^*_{CN} \leftarrow \pi_{CN}$ transition in CCl_4, since it appears below the 200 nm region. The UV spectrum therefore indicates that structure **2b** is also present in solution. Such an interpretation is supported by the UV spectrum of **3**. In the spectrum of this compound where no tautomerization is possible, only a single absorption maximum of 264 L mol^{-1} cm^{-1} at 216 nm is present as was the case in **1**. Because the conjugated **2b** form is expected to absorb strongly its concentration in solution must be very small which would explain the observed absorption behaviour. Moreover, the presence of this enamine form cannot be determined in ^{13}C- and ^{1}H-NMR spectra, which confirms a very high percentage of **2a** tautomer present in solution.

Recently Dianxun *et al.*[31] proposed the existence of a linear correlation between the lowest ionization energy (from PES) and the chemical shift (from ^{13}C-NMR) for the carbon atom in the –N≡C group of alkyl isocyanides. Other attempts to correlate chemical NMR δ shifts with the size of a molecule as well as with the PES data are also known.[32]

We have not found an analogous relationship between the first ionization energies and chemical shifts in compounds **1**–**3**. In all other bisoxazolines studied here, the strong overlap of benzene ring ionizations in the low energy region of the PES prevented the exact measurement of the lowest oxazoline ring ionization energy from being obtained (see Table 2, Fig. 2). The chemical shifts are related to electrons "belonging to individual atoms", whereas the ionization energies determined by PES are related to electron distributions which are delocalized over all atoms in the molecule, within the framework of Koopmans' approximation.[33] Therefore a good correlation can be expected only if the ionization takes place from an orbital which is localized (*e.g.* lone pair) on an atom whose chemical shift is being correlated, or at least on the neighbouring atom. In addition, the observation time scales in the two methods are different: the NMR yields information about time averaged mean conformations, whereas PES can provide insight into momentary conformations.[34]

Table 4 Total atomic charges as derived by Mulliken population analysis from *ab initio* 6-31G* for compounds **1**–**3**, and corresponding ^{13}C-NMR chemical shifts

Compound	Total atomic charges, μ		δ_μ
1	C(2)	0.618	164.180
1	C(4)	−0.029	66.130
1	C(5)	−0.183	53.390
1	CH_3	−0.538	12.300
2	C(2)	0.662	161.550
2	C(2)-*C*	−0.446	28.060
2	C(4)	−0.021	75.610
2	C(5)	−0.013	68.980
2	C(4)-*C*	−0.038	26.690
3	C(2)	0.714	168.690
3	C(2)-*C*	−0.201	33.700
3	C(4)	−0.019	75.160
3	C(5)	−0.011	68.840
3	C(4)-*C*	−0.038	26.720

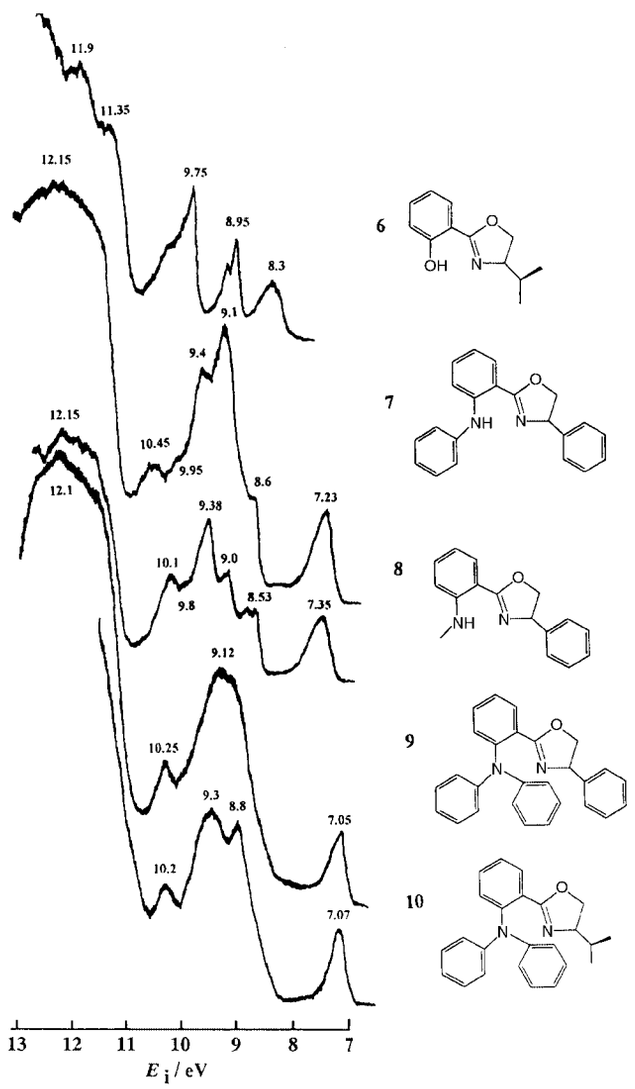

Fig. 3 He(I) PE spectra of **6**–**10**.

In our attempt to find a connection between observed chemical shift and charge densities within the molecule we have used *ab initio* 6-31G* calculations for **1**–**3** in spite of the fact that there is no unique way to apportion total electron (charge) density amongst individual atoms in a molecule.[35] Nonetheless the population analysis can still provide valuable insights.[36] The values of ^{13}C-NMR chemical shifts and corresponding *ab initio* total atomic charges derived from a Mulliken population analysis for carbon atoms in **1**–**3** as assigned in the structural formula (Scheme 2) below are given in Table 4. They correlate quite well ($r = 0.947$, $\sigma = 0.127$, see Fig. 4).

Table 5 Vertical ionization energies (E_i/eV) and orbital energies for highest occupied levels for **6**–**10**[a]

Compound	E_i/eV	$-\varepsilon_i$/eV (PM3)
6	8.3	9.04 π^s_1
	8.95	9.69 π^a_1, π_{CN}
	9.75	10.64 π_{CN}, π^a_1
	10.15	10.89 n_N
7	7.23	8.68 π^s_1
	8.6	9.599 π^s_2
	8.8	9.74 π^a_2
		9.83 π^a_1
	9.1	9.93 π_{CN}, π^a_1
		10.0 π_{CN}, π^a_1
		10.07 π^a_1, π_{CN}
	10.45	10.66 n_N
8	7.35	9.08 π^s_1
	8.53	9.51 π^s_2
	9.0	9.68 π^a_2
	9.38	9.96 π_{CN}, π^a_1
		10.04 π_{CN}, π^a_1
	9.8	10.33 π^s_1
	10.1	10.52 n_N
9	7.05	8.61 π^s_1
	8.6	9.52 π^s_2
	8.8	9.7 π^a_2
		9.72 π^s_1, $\pi^s_{1'}$
	9.0	9.77 $\pi^s_{1''}$
		9.81 $\pi^s_{1'}$, $\pi^s_{1''}$
	9.12	9.89 π_{CN}, π^a_1
		9.89 π^a_1
		10.14 π_{CN}, π^a_1
	10.25	10.6 n_N
10	7.07	8.48 $\pi^s_{1'}$
	8.6	9.66 π^s_1, $\pi^s_{1'}$
	8.8	9.68 π^a_1, $\pi^a_{1'}$
		9.79 π^s_1
	9.3	9.84 π_{CN}, π^s_1
		9.99 $\pi^s_{1'}$, π^s_1
		10.11 π^a_1, π_{CN}
	10.2	10.52 n_N

[a] π^s_b, π^a_b refer to symmetric and antisymmetric benzene orbitals from phenyl substituents located at position 2 and 4 of oxazoline specified by subscript 1 and 2, respectively. Subscripts 1′ and 1″ refer to additional phenyl groups in the *n*-phenylamine substituent.

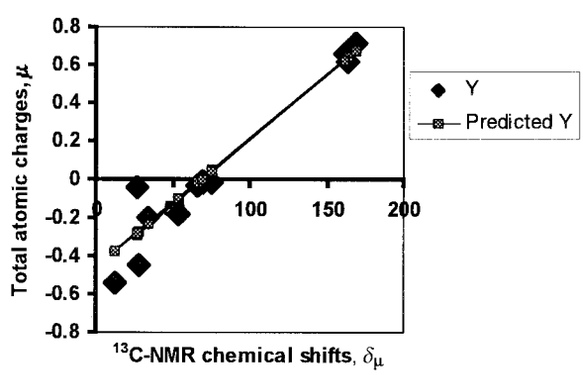

Fig. 4 Correlation of Mulliken atomic charges obtained from *ab initio* 6-31G* calculations.

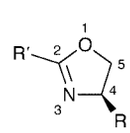

Scheme 2

In the PE spectra of **4** and **5** we have observed, in addition to ionizations from $\pi_{C=N}$ and n_N orbitals, other bands which generate final, complex FC envelopes (see Fig. 2, Table 2). According

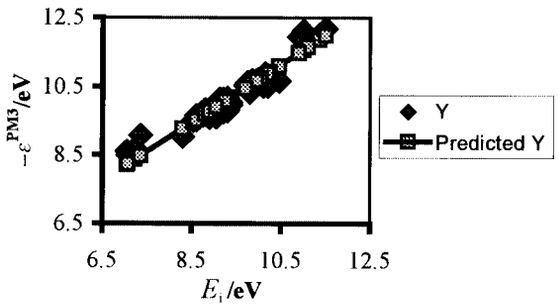

Fig. 5 Correlation of experimental ionization energies and semi-empirical PM3 orbital energies.

to PM3 calculations the shoulders on the low energy side are interpreted as "pure" ionizations from two π^s and two π^a MO of both benzene rings which have energies comparable to $\pi_{C=N}$ bisoxazoline orbitals. The broad 'hump' with a maximum at 10.05 eV is ascribed to ionization from both n_N orbitals. The effect of the additional two methyl groups in **5** is manifested by inductive destabilization of the bands which is reminiscent of the effect observed on going from **3** to **2**.

Mono-oxazolines

The electronic structures of the substituted oxazolines **6**–**10** have been studied using PE spectroscopy (see Fig. 3) and PM3 MO calculations (Table 5). The low energy bands (7.05–7.36 eV) in compounds where oxazoline is connected to mono-, di- or triphenylamine are attributed to molecular orbital(s) of (*n*)-phenylamine origin (*n* = number of phenyl groups), whereas the ionization of π_{CN} and n_N orbitals gives rise to bands at considerably higher energies (~9–10 eV and slightly above 10 eV, respectively). This assignment is supported by the higher ionization energy in **6** (8.3 eV), which has a phenol instead of an (*n*)-phenylamine substituent. Such an interpretation is consistent with the PE spectra of bisoxazolines where the bands corresponding to $\pi_{C=N}$ ionizations appear at 9–9.3 eV and those from nitrogen lone pair ionizations n_N appear at 10 eV. The scattering of points in Fig. 5 is small and is thus indicative of a good linear correlation between experimental ionization energies and PM3 calculations results ($r = 0.96$, $\sigma = 0.22$).

Conclusion

The electronic structure of some mono- and bisoxazolines has been determined on the basis of photoelectron spectra and quantum chemical calculations. The information provided by UV and ^{1}H- and ^{13}C-NMR spectra was also considered.

According to PE spectra, ^{1}H- and ^{13}C-NMR spectra, the **2a** tautomeric form of bisoxazoline **2** is the dominant species in the gas phase as well as in solution. UV spectra indicate only a small amount of **2b** to be present in solution.

The ^{13}C-NMR chemical shifts of bisoxazolines **1**–**3** correlate well with total atomic charges derived from Mulliken population analysis based on *ab initio* 6-31G* calculations.

The lowest energy bands in **1**–**3** are assigned to π_{CN} and to n_N orbital ionizations, whereas in phenol and (*n*)-phenylamine-substituted monooxazolines **6**–**10** the same bands are attributed to π orbitals of phenylamine or phenol origin.

References

1 A. Pfaltz, *Acc. Chem. Res.*, 1993, **26**, 339.
2 M. P. Doyle, in *Catalytic Asymmetric Synthesis*, Ed. I. Ojima, VCH, New York, 1993, pp. 63–99.
3 X.-Y. Wu, X.-H. Li and Q.-L. Zhou, *Tetrahedron: Asymmetry*, 1998, **9**, 4143.
4 S. Đaković, L. Tumir-Liščić, S. I. Kirin, V. Vinković, Z. Raza, A. Šuste and V. Šunjić, *J. Mol. Catal.*, 1997, **118**, 27.
5 S. G. Nelson, *Tetrahedron: Asymmetry*, 1998, **9**, 357.
6 D. A. Evans, C. S. Burgey, N. A. Paras, T. Vojkovsky and S. Tregaj, *J. Am. Chem. Soc.*, 1998, **120**, 5824.
7 Y. Motoyama, H. Narusawa and H. Nishiyama, *Chem. Commun.*, 1999, 131.
8 A. Lightfoot, P. Schneider and A. Pfaltz, *Angew. Chem., Int. Ed. Engl.*, 1998, **37**, 2897.
9 G. Chelluci, S. Medici and A. Saba, *Tetrahedron: Asymmetry*, 1997, **8**, 3183.
10 G. Chelucci, *Tetrahedron: Asymmetry*, 1997, **8**, 2667.
11 K. Nordström, E. Macedo and C. Moberg, *J. Org. Chem.*, 1997, **62**, 1604.
12 U. Bremberg, F. Rahm and C. Moberg, *Tetrahedron: Asymmetry*, 1998, **9**, 3437.
13 G. Chelucci, S. Medici and A. Saba, *Tetrahedron: Asymmetry*, 1999, **10**, 543.
14 U. Bremberg, M. Larhed, C. Moberg and A. Hallberg, *J. Org. Chem.*, 1999, **64**, 1082.
15 Y. Uozumi, H. Kyota, M. Ogasawara and T. Hayashi, *J. Org. Chem.*, 1999, **64**, 1620.
16 Y. Jiang, Q. Jiang and X. Zhang, *J. Am. Chem. Soc.*, 1998, **120**, 3817.
17 M. Bandini, P. G. Cozzi, L. Negro and A. U. Ronchi, *Chem. Commun.*, 1999, 39.
18 Purchased from Aldrich.
19 L. Tumir, BSc Thesis, University of Zagreb, 1995.
20 M. J. Frisch, G. W. Trucks, H. B. Schlegel, P. M. W. Gill, B. G. Johnson, M. A. Robb, J. R. Cheeseman, T. Keith, G. A. Petersson, J. A. Montgomery, K. Raghavachari, M. A. Al-Laham, V. G. Zakrzewski, J. V. Ortiz, J. B. Foresman, J. Cioslowski, B. B. Stefanov, A. Nanayakkara, M. Challacombe, C. Y. Peng, P. Y. Ayala, W. Chen, M. W. Wong, J. L. Andres, E. S. Replogle, R. Gomperts, R. L. Martin, D. J. Fox, J. S. Binkley, D. J. Defrees, J. Baker, J. P. Stewart, M. Head-Gordon, C. Gonzalez and J. A. Pople, GAUSSIAN94, Revision D.4, Gaussian, Inc., Pittsburgh, PA, 1995.
21 L. Klasinc, B. Kovač and B. Ruščić, *Kem. Ind.*, 1974, **10**, 569.
22 Z. Raza, S. Đaković, V. Vinković and V. Šunjić, *Croat. Chem. Acta*, 1996, **69**, 1545; B. Kovač, L. Klasinc, Z. Raza and V. Šunjić, unpublished results.
23 H. Bock and R. Dammel, *Chem. Ber.*, 1987, **120**, 1971; C. N. R. Rao and P. K. Basu, *Ultraviolet Photoelectron Spectroscopy of Heterocyclic Compounds*, in *Physical Methods in Heterocyclic Chemistry*, Ed. R. R. Gupta, J. Wiley & Sons, New York, 1984.
24 N. T. Anh and F. Maurel, *New J. Chem.*, 1997, **21**, 861; M. Peräkylä and T. A. Pakkanen, *J. Chem. Soc., Perkin Trans. 2*, 1995, 1405.
25 R. W. Alder, R. J. Arrowsmith, A. Casson, R. B. Sessions, E. Heilbronner, B. Kovač, H. Huber and M. Taagepera, *J. Am. Chem. Soc.*, 1981, **103**, 6137.
26 I. Novak and B. Kovač, *Heteroatom Chem.*, 1995, **6**, 29.
27 M. W. Wong, R. Leung-Toung and C. Wentrup, *J. Am. Chem. Soc.*, 1993, **115**, 2465.
28 M. Maus, W. Rettig, D. Bonafoux and R. Lapouyade, *J. Phys. Chem. A*, 1999, **103**, 3388.
29 D. Chen, R. Sadygov and E. C. Lim, *J. Phys. Chem.*, 1994, **98**, 2018.
30 R. S. Mulliken, *J. Am. Chem. Soc.*, 1952, **74**, 811.
31 W. Dianxun, Q. Ximei and Z. Shijun, *Chem. Phys. Lett.*, 1996, **262**, 776.
32 Y. Miyashita, T. Okuyama, H. Ohsako and S. Sasaki, *J. Am. Chem. Soc.*, 1989, **111**, 3469; O. Exner, *J. Phys. Org. Chem.*, 1997, **10**, 797; L. Klasinc, Lj. Paša-Tolić, D. Vikić-Topić, J. V. Knop and S. P. McGlynn, *Int. J. Quantum Chem.*, 1997, **63**, 797.
33 T. Koopmans, *Physica*, 1934, **1**, 104.
34 H. Bock, K. Ruppert, C. Näther, Z. Havlas, H.-F. Herrmann, C. Arad, I. Gëbel, A. John, T. Vaupel and B. Solouki, *Angew. Chem., Int. Ed. Engl.*, 1992, **31**, 550; M. Mohraz, W. Jian-qi, E. Heilbronner, A. Solladié-Cavallo and F. Matloubi-Moghadam, *Helv. Chim. Acta*, 1981, **64**, 97.
35 D. Bergmann and J. Hinze, *Angew. Chem., Int. Ed. Engl.*, 1996, **35**, 150.
36 E. Tajkhorshid, B. Paizs and S. Suhai, *J. Phys. Chem. B*, 1997, **101**, 8021.

Paper 9/06031F